



Obrabotka metallov -

Metal Working and Material Science





Journal homepage: http://journals.nstu.ru/obrabotka_metallov





Study of the kinetics of forming of spherical sliding bearing parts made of corrosion-resistant steels by die forging of porous blanks

Badrudin Gasanov^{a,}, Nikolai Konko^b, Sergey Baev^c*

Platov South-Russian State Polytechnic University (NPI), 132 Prosveshcheniya st., Novocherkassk, 346428, Russian Federation

^a  <https://orcid.org/0000-0001-7610-4541>,  gasanov.bg@gmail.com; ^b  <https://orcid.org/0009-0003-8098-2226>,  konko2013@mail.ru;

^c  <https://orcid.org/0009-0006-5527-6620>,  baev93@mail.ru

ARTICLE INFO

Article history:

Received: 13 March 2024

Revised: 08 April 2024

Accepted: 13 April 2024

Available online: 15 June 2024

Keywords:

Die forging

Powder blank

Relative density

Coefficient of contact friction

Simulation

Strain state

Acknowledgements

Access to QForm cloud license is provided by the Department of Pressure Processing Technologies of Bauman Moscow State Technical University and QuantorForm LLC.

ABSTRACT

Introduction. Spherical powder sliding bearings are widely used in various branches of mechanical engineering. Therefore, the development of a promising method of production of spherical sliding bearing parts from powders of corrosion-resistant steels with specified properties is an urgent task. **Purpose of work:** is to study the kinetics of forming during cold die forging of spherical sliding bearing parts from stainless steel powder blanks, and to assess the effect of the chemical composition of lubricants and the design of the pressing tool on the structure and properties of the bearing outer ring. Materials from sprayed powders of stainless chromium-nickel steels obtained by cold die forging of sintered blanks coated with lubricants are studied in the work. The following **research methods** were used: mechanical tensile testing, metallographic studies and cold die forging process simulation. **Results and its discussion.** It is revealed that the resistance and work of deformation, as well as the kinetics of forming of the outer ring of the spherical sliding bearing are influenced by chemical composition of powders and lubricants, microstructure and mechanical properties of the blank material, configurations of the end surfaces of punches. The top and bottom edges of the outer bearing are most intensively sealed when the punch faces are made with a chamfer angle of 30–40 degrees. With an increase in the relative strain degree by height up to 0.30–0.35 its residual porosity amounted to 0.5–2.0 %. The features of definition of strain state and calculation of strain energy in the implementation of the offered method and the choice of technological parameters of the cold die forging process of sliding bearings parts are shown. A simple method for calculating and experimentally determining the coefficient of contact friction in the process of cold die forging of porous stainless steel blanks is developed, which allows to establish the effect of lubricant composition on the strain resistance at different values of the degree of radial deformation and to develop optimal methods of cold die forging of porous blanks in the production of parts of different complexity.

For citation: Gasanov B.G., Konko N.A., Baev S.S. Study of the kinetics of forming of spherical sliding bearing parts made of corrosion-resistant steels by die forging of porous blanks. *Obrabotka metallov (tekhnologiya, oborudovanie, instrumenty) = Metal Working and Material Science*, 2024, vol. 26, no. 2, pp. 127–142. DOI: 10.17212/1994-6309-2024-26.2-127-142. (In Russian).

Introduction

Depending on the configuration, dimensions, mechanical and technological properties of materials, various methods of hot and cold die forging of powder products are used [1–3, etc.]. When die forging parts with curvilinear elements, characteristic, for example, of spherical sliding bearings, levers, fine-modular gears and others, it is advisable to design powder blanks taking into account the plasticity of the material, forming schemes, as well as the requirements for the die forged products [4–8]. Particular attention is paid to the design and optimization of technological parameters of powder blanks production, since powder metallurgy methods guarantee greater metal savings, productivity growth, energy costs reduction, etc.

* Corresponding author

Gasanov Badrudin G. D.Sc. (Engineering), Professor
Platov South-Russian State Polytechnic University (NPI),
132 Prosveshcheniya st.,
346428, Novocherkassk, Russian Federation
Tel.: +7 928 227-07-16, e-mail: gasanov.bg@gmail.com

Technological possibilities of cold or hot die forging of powder products can be successfully realized in the presence of scientific, design and technological generalized results, the use of which will provide the required quality and properties of the obtained materials, density distribution by volume, durability and cost of tooling [9–12]. This makes it necessary to determine the stress-strain state during cold or hot die forging of powder blanks of different configurations and materials. One of the ways to solve boundary value problems in the theory and technology of hot and cold die forging of powder products is to determine the kinematic parameters in characteristic cross-sections of blanks at different stages of its forming in order to establish the relationship between the strain component and stresses, as well as to identify the allowable values of strains, nucleation and development of cracks during die forging [13–17]. Various simulation models and programs can be used for this purpose [18, 19].

The purpose of the work is to study the influence of tool design, lubricant composition and method of manufacturing sintered blanks from corrosion-resistant steel powders on the kinetics of forming during cold die forging of spherical sliding bearing parts.

Research methods

One of the design options of the non-separable spherical sliding bearing is shown in (Fig. 1). The manufacturing technology of such sliding bearings, often used in aviation industry, is not described in the publications available to us. However, some requirements for it have been formulated: reliable operation in various conditions under the action of high radial and axial loads, minimum wear and friction coefficient, predictable operational life and others. Such friction units are made of corrosion-resistant steels with the use of special lubricants. Inner rings of the bearing unit are made of steel *AISI 52100*, after maintenance its hardness is HRC 58–61. The outer ring is made of powders of corrosion-resistant steels *304L-AW-100* of “Höganäs” (Sweden) and *0.12C-18Cr-10Ni-Ti* of domestic production, as well as components and ligatures (Table 1).

To study the mechanical and technological properties of porous blanks, circular (*GOST 26529–85* and *GOST 18227–98*) and prismatic (*GOST 1497–84*) tensile test specimens were made. Specimens for research were pressed on a hydraulic press *HPM–60L* in a cylindrical mold with a floating matrix under pressure from 200 to 800 MPa. Part of the pressings was sintered in a laboratory furnace with carbide-silicon heaters in dissociated ammonia, another part was sintered at 1,150 °C for 1.5–2 hours in a vacuum electric furnace *VSI–16–22–U*.

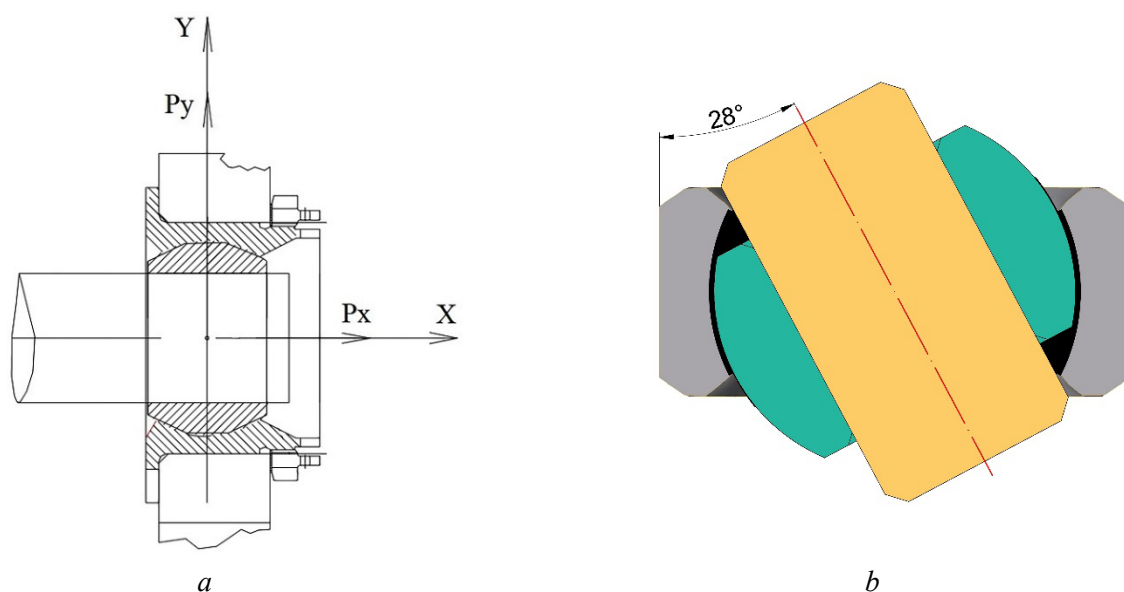


Fig. 1. Spherical sliding bearing:

a – sections of friction unit; *b* – maximum rotation angle of the inner bearing

Chemical composition of the powder materials used

Material	Chemical composition, %											
	Si	Cu	Mn	Ni	Ti	P	Cr	S	C	V	W	Fe
0.12C-18Cr-10Ni-Ti	0.8	0.3	2.0	10.0	0.7	0.035	18.0	0.020	0.12	2.0	0.2	Bal.
304L-AW-100	0.87	–	0.2	10.63	–	0.017	18.18	0.01	0.03	–	–	Bal.
18Cr-4Ni-3Cu	2.0	3.0	–	4.0	–	0.03	18.0	0.05	2.0	–	–	Bal.

Porosity of sintered specimens was determined by hydrostatic weighing and varied in the range of 12–25 %, the coordinate grid on the sintered blanks was applied on a CNC laser engraver *JL-F20W* with a laser power of 15 W with a step of 0.5 mm (Fig. 2).



Fig. 2. Section of the outer ring of a spherical bearing with a coordinate grid after punching:

a – with a chamfer; *b* – without a chamfer

Molybdenum disulfide (*TU48-19-133-90*), pencil graphite (*GOST23463-79*) and polytetrafluoroethylene (PTFE) (*GOST 10007-80*) were used to study the influence of a lubricant composition on the contact friction coefficient and deformation resistance. To simulate cold die forging of the outer ring of the spherical sliding bearing outer ring according to the scheme shown in (Fig. 3), we used the *QForm* program, based on a hybrid approach that combines finite element and volume methods, providing fast and accurate calculation of porosity changes and stress-strain state of the workpiece at all stages of forming [19].

The process of forming the spherical part of the inner surface of the ring **5** by cold forming (two-sided pressing) and the influence of the design of the end surfaces of punches **2** and **6** on the kinetics of deformation of porous cylindrical blank were investigated using a mold, the scheme of which is shown in (Fig. 3).

Results and their discussion

Studies have shown that the strain resistance force P_d of powder blank **5** during cold forming of sintered blanks is influenced not only by the mechanical properties of the material, but also by the configuration of the forming surface of punches **2** and **6** (Fig. 3). By simulating in the *QForm* program the process of deformation of a blank with an initial relative density of 0.8 mm, a height of 14.5 mm, an outer diameter of 25 mm and a wall thickness of 2.75 mm according to the double-sided pressing scheme, it was found that at the stage of compaction of the porous molding (i.e. that is, with its relative degree of strain $\epsilon_z \leq 0.08 \dots 0.1$), the force P_d insignificantly depends on the angle of the internal chamfer (Fig. 4, *a*). In the case of using punches with a flat end face ($\alpha_f = 0$) and with an increase in ϵ_z above 0.15...0.16, the strain resistance force increases almost twice as compared to when $\alpha_f = 40-50$ deg (Fig. 4, *b*). In particular, if the cone angle corresponds to the angle of rotation of the spherical bearing by 45° , then the strain resistance force of the porous blank at $\epsilon_z = 0.25$ does not exceed 50 kN, while at $\alpha_f = 0$ the force P_d is equal to 200 kN. Similarly, the angle α_f affects the strain energy.

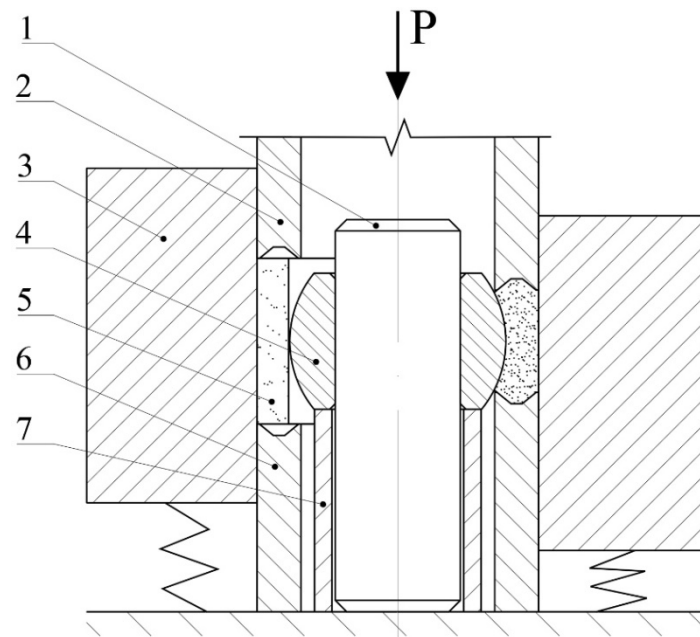
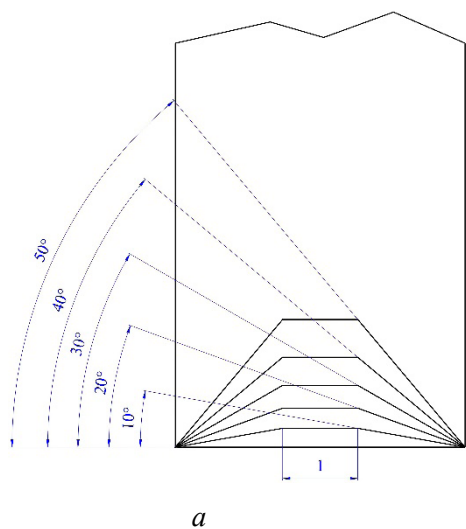
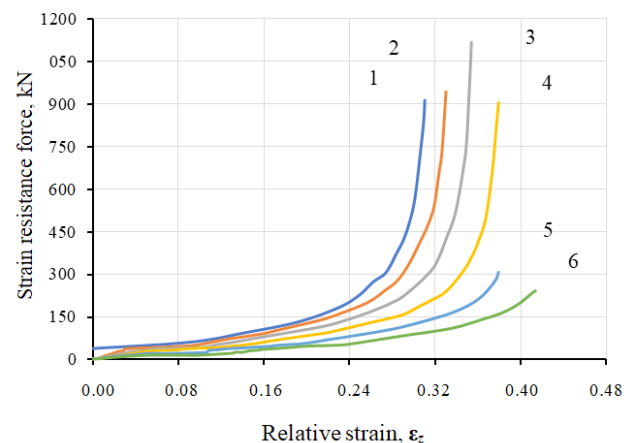


Fig. 3. Press tool for cold die forging:

1 – rod; 2, 6 – upper and lower punches; 3 – floating die;
4 – internal (spherical) bearing of the hinge unit; 5 – powder blank;
7 – fixing lower punch



a



b

Fig. 4. Influence of relative strain of the porous blank on the strain resistance depending on the chamfer angle α_{ch} at the end of the upper and lower punches, deg:

1 = 0; 2 = 10; 3 = 20; 4 = 30; 5 = 40; 6 = 50

The *QForm* program allows not only to establish the dependence of strain resistance and evaluate the work of active forces, but also to simulate the process of cold forming of a porous blank at any moment of time. As an example, (Fig. 5) shows the density distribution, stress field and accumulated (effective) deformation at different values of ϵ_z .

After the pressure is removed during cold forming, the bearing outer ring is tightly seated in the forming seat of the matrix as a result of elastic aftereffects (Fig. 3). Therefore, a certain force is required to push it out of the matrix, which depends on the initial and residual porosity of the ring, the specific work of cold deformation, the characteristics of lubricants, etc. In this case, the outer diameter of the outer ring of the bearing after ejection increased by about 0.03 mm relative to the diameter of the matrix, and the radial increase in the inner diameter of the ring as a result of elastic aftereffect was about 0.01 mm, which is sufficient in the presence of lubricant for free rotation of the inner ring relative to the outer ring.

Since in the process of molding the inner spherical surface of the outer ring as a result of bilateral sintered blank upsetting, the relative displacement of metal on the surface of the inner ring is insignificant, in the process of experimental studies did not observe adhesion or splicing of the material of the outer and inner rings of the bearing.

When die forging porous blanks, it is necessary to identify the distribution of material density in each stage. The top and bottom edges of the outer bearing are most intensively compacted when the punch faces are produced with a chamfer angle of 30–40 deg. With increasing ε_z up to 0.30–0.35, residual porosity in these zones (have dark orange and red background) does not exceed 0.5–2.0 % (Fig. 5, *a*).

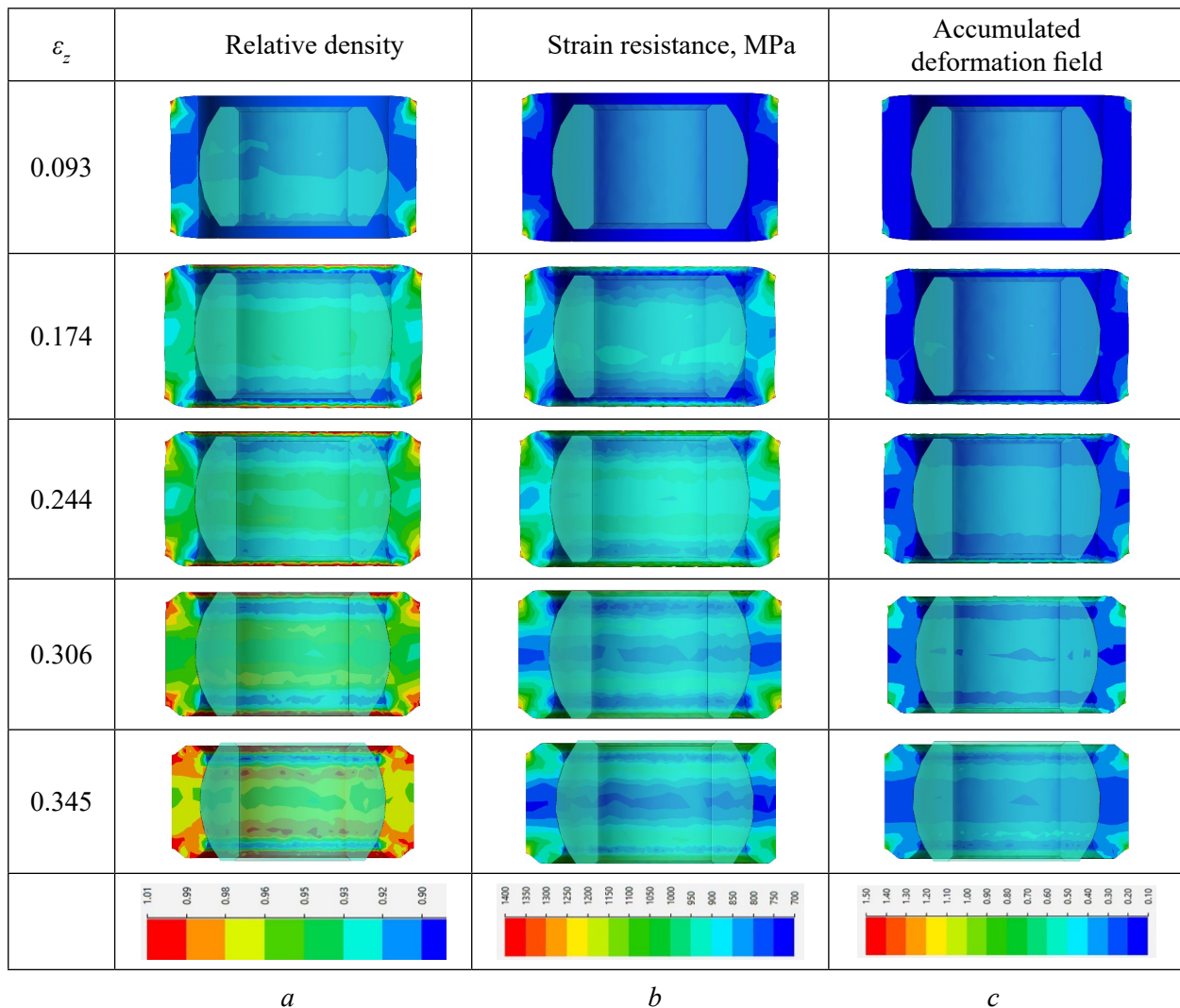


Fig. 5. Volume distribution of relative density (*a*), specific strain resistance (*b*) and accumulated deformation field (*c*) during simulation of die forging of a porous blank in *QForm* program

To experimentally evaluate the distribution of residual porosity in the bearing outer ring after cold forming, microsections were used. (Figs. 6, *a* and 6, *b*) show the microstructure of the unetched microsections of two areas of the meridian section of the ring with maximum (Fig. 5, *a*, has a red background) and minimum (Fig. 5, *a*, has a bluish background) relative density. Porosity in these zones does not exceed 1–2 and 7–9 %, respectively. These studies show a fairly good agreement between the results of simulation and experiment in estimating the density of the material.

In the cold forming process, the relative density θ increases in proportion to the accumulated strain (Fig. 5, *c*). For example, θ of the material in the region of the inner spherical surface of the ring, depending on the height and degree of strain ($\varepsilon_z = 0.33$ –0.35) ranges from 0.92–0.98. Since the central inner part of the blank is compacted to a lesser extent than the ends, on the one hand, it allows to increase the amount

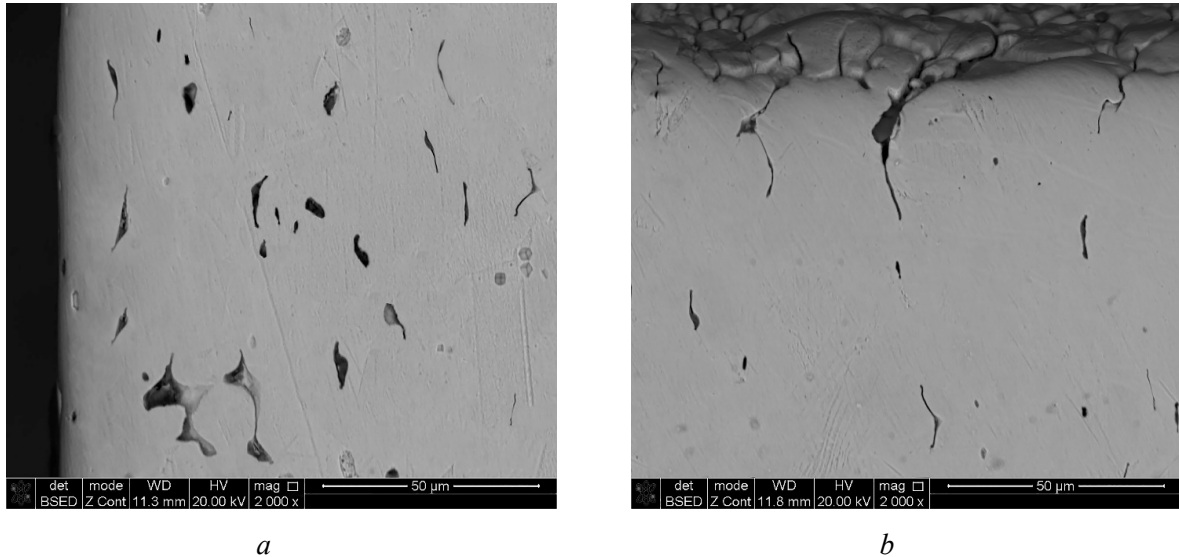


Fig. 6. Microstructure of unetched microsection of the bearing outer ring areas with porosity, %:
a – 8–9; b – 1–2

of solid lubricant concentrated in the pores of the metal matrix, respectively, to reduce the coefficient of friction between the spherical bushing and the outer ring of the bearing, and on the other hand, relatively large residual porosity reduces the ultimate strength of the ring material and the limit values of axial loads.

In the case of using punches with a flat end surface (Fig. 7, a), the maximum relative density (0.98–0.99) was obtained in the zones of contact of punches with the end surface of the workpiece, where the intensity of plastic deformation of the material is significantly greater than in the central zone. Such areas of the blank after die forging are highlighted in (Fig. 7, a) in red color. However, the work of active forces and strain resistance in this case is somewhat greater than when using punches with internal chamfers (Fig. 7, b).

The *QForm* program allows modeling a rectangular grid (Fig. 2, a), which is initially two-dimensional, but with some assumptions it is possible to calculate parameters for a three-dimensional grid with a certain error, provided that the radius R is constant at any point of the section. The displacements of nodal points were determined by the total displacement of each grid element, so we calculated linear and shear deformations based on the changes in linear dimensions and shape of a particular grid element (Fig. 2, b). Taking into account the results of simulation and using the thin section methodology, we selected representative elements by height and radius of the blank (Fig. 8, d) with coordinates $K_h = h_i/h_o$ and $K_r = r_i/r_o$. As an example, the values of ε_{xx} , ε_{yy} and ε_{xy} calculated by known formulas [20, 21] are shown in (Fig. 8).

The nature of the dependencies of ε_{xx} , ε_{yy} and ε_{xy} on the radius of the outer ring of the hinge, determined by the deformation of the coordinate grid and modeling by the *QForm* program, practically does not differ (Fig. 8). However, the values of component ε_{xx} , ε_{yy} and ε_{xy} calculated from the increment of the coordinate points of the grid are slightly larger than those determined by simulation.

Assuming that the strain energy from the inner spherical bearing is insignificant, the strain energy balance equation is written in the following form:

$$A_a = A_d + A_f, \quad (1)$$

where A_a is the work of active forces; A_d is the strain energy; A_f is the work of external friction forces.

Work of (external) active deformation forces:

$$A_a = P_d \Delta h, \quad (2)$$

where P_d is the strain resistance force of the blank; Δh is the change in height of the blank.

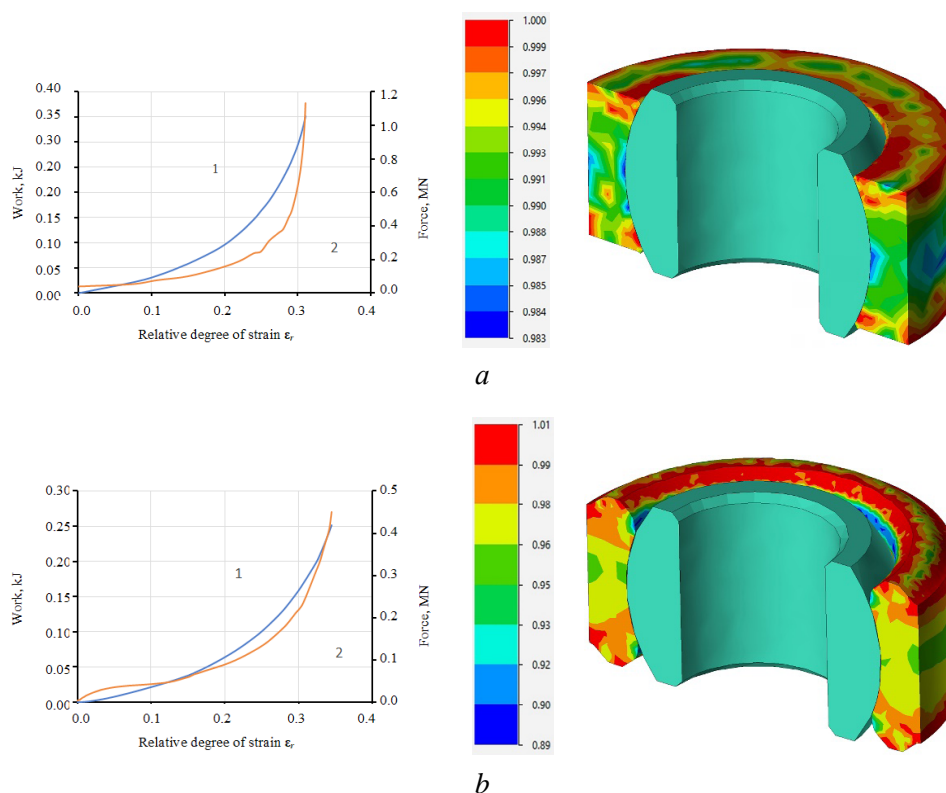


Fig. 7. Simulation in the *QForm* program of plastic strain of a porous bushing being settled on a spherical bearing of a hinge unit:

1 – strain resistance force; 2 – strain energy

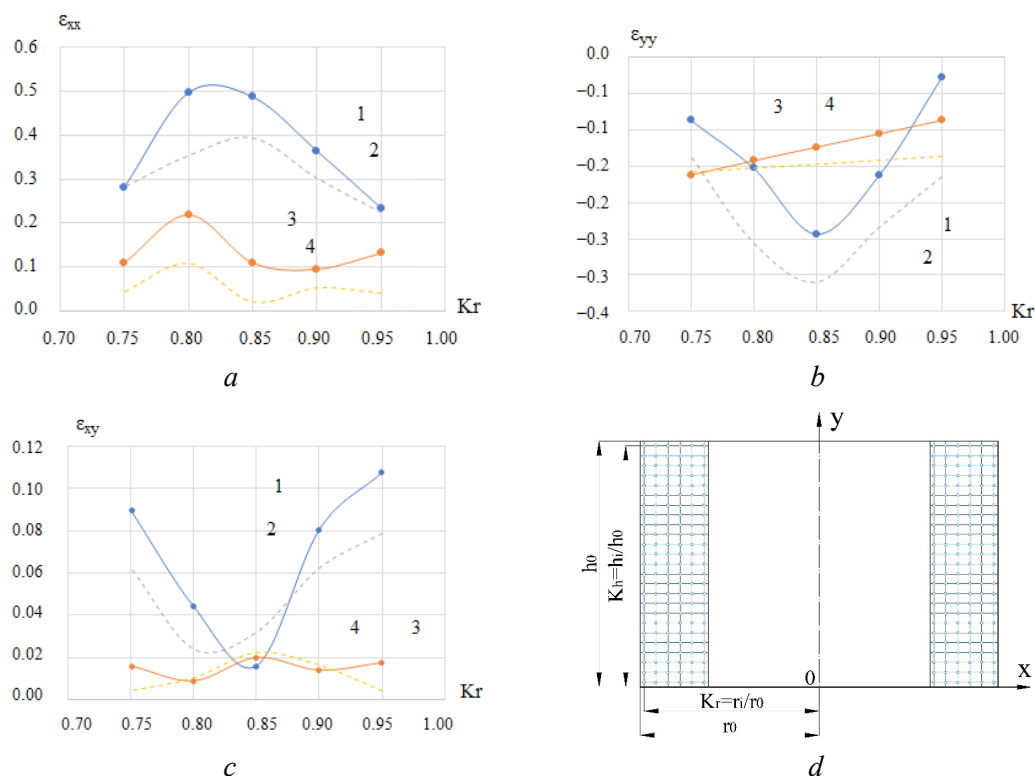


Fig. 8. Distribution of the relative strain degree of the ring section elements ϵ_{xx} (a), ϵ_{yy} (b) and ϵ_{xy} (c) with coordinates $K_h = 0.5$ (3; 4) and 0.85 (1; 2) as a function of K_r , determined:

1 and 3 – experimentally; 2 and 4 – by simulation

If the stress-strain state at each stage of molding a porous blank is known, the stress and strain intensity can be determined. Since in the plastic state the stress intensity is constant $\sigma_i = \sigma_s$ and the increment of strain work [20–22]:

$$dA_d = \iiint \sigma_s \cdot \varepsilon_i \cdot dV, \quad (3)$$

where dV is the volume increment of the displaced metal; σ_s is the yield strength of the porous blank material; ε_i is the strain intensity.

Fig. 9 shows, as an example, the strain intensity distribution of the top and middle layer of the blank, calculated using the following equation:

$$\varepsilon_i = \frac{\sqrt{2}}{3} \sqrt{(\varepsilon_{xx} - \varepsilon_{yy})^2 + \frac{3}{2} \gamma_{xy}^2}. \quad (4)$$

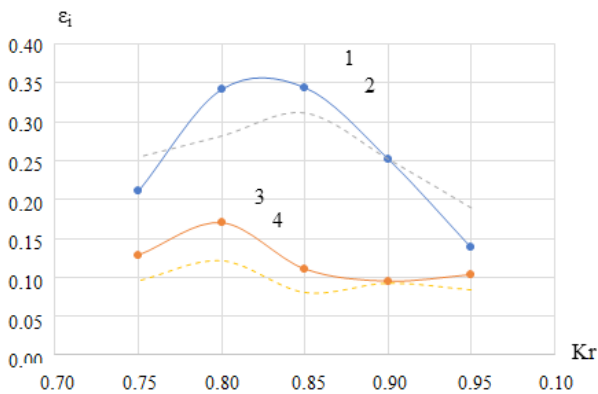


Fig. 9. Dependence of strain intensity ε_i of thin sections with $K_h = 0.5$ (3, 4) and 0.85 (1, 2) of the sintered blank on its reduced radius K_r , determined:

1 and 3 – experimentally; 2 and 4 – by simulation

The incremental work of contact friction forces was generally represented as follows:

$$dA_f = \tau_c \cdot dF_c, \quad (5)$$

where τ_c is the tangential stresses on the contact surfaces; dF_c is the increment of the contact area “tool-blank”.

If the contact friction stress is known, the following formula has been proposed to determine the work of contact friction forces [20]:

$$A_f = \tau_c \iint \sqrt{u_2^2 + v_2^2 + w_2^2} dF. \quad (6)$$

The specific deformation force of the porous blank was determined from the simulation results and according to the formula [22]:

$$p = \sigma_s + \frac{1}{3} \cdot \tau_c \cdot \frac{(D - d)}{h}, \quad (7)$$

where σ_s is the material yield strength; τ_c is the tangential stresses on the contact surfaces; D and d are the bushing outer and inner diameters.

The equation for determining the stress τ_c on the tangent surface of the tool and the porous blank has the following form [9, 23]:

$$\tau_c = \mu_c \cdot \sigma_s \cdot \sqrt{(1 - \Theta)^3}, \quad (8)$$

where μ_c is the contact friction coefficient; Θ is the relative density of the blank.

Substituting expression (7) into formula (6), we find:

$$p = \sigma_s + \frac{1}{3} \cdot \left(\mu_c \cdot \sigma_s \cdot \sqrt{(1 - \Theta)^3} \right) \cdot \frac{(D - d)}{h} \quad (9)$$

Solving dependencies (8) and (5) together, we determined the work of active forces:

$$A_a = \frac{\pi}{4} (D^2 - d^2) \left[\sigma_s + \frac{1}{3} \left(\mu_c \sigma_s \sqrt{(1 - \Theta)^3} \right) \frac{(D - d)}{h} \right] \Delta h. \quad (10)$$

Yield strength σ_s of sintered corrosion-resistant steel depends on many factors: chemical composition, structure, porosity, concentration and configuration of foreign inclusions, etc. Various formulas are used to evaluate the effect of porosity on the yield strength of sintered structural materials. In particular, the following expression was proposed in [18]:

$$\sigma_s = \sigma_{so} \frac{2(1 - \Theta)^2}{\sqrt{4 - 3\Theta}}, \quad (11)$$

where σ_{so} is the yield strength of compact material.

For compact chromium-nickel steels of the austenitic class offset yield strength is ($\sigma_{0.2}$) is 250–450 MPa. Therefore, σ_s of sintered steels, the composition of which is indicated in Table 1, were determined experimentally according to *GOST 1497–84*, using prismatic tensile test specimens.

Table 2 shows some mechanical properties and porosity of prismatic specimens after sintering at 1,150 °C, 1.5 hours. The ultimate strength of specimens sintered in dissociated ammonia is very low, because even in the case of sintering in the backfill chromium is intensively oxidized, especially at the boundaries of powder particles, due to the interaction not only with oxygen contained in the protective medium, but also with oxygen slammed in the pores of the blank.

Table 2

Physical and mechanical properties of chromium-nickel sintered corrosion-resistant steels

Sintering medium	Dissociated ammonia			Vacuum		
	Backfill SiO ₂		Backfill SiO ₂ +Al ₂ O ₃			
Powder grade	0.12C-18Cr-10Ni-Ti	304L-AW-100	18Cr-4Ni-3Cu	0.12C-18Cr-10Ni-Ti	304L-AW-100	18Cr-4Ni-3Cu
σ_u , MPa	29.7	45.59	45.10	243.59	237.84	144.15
δ , %	0.13	0.11	0.60	7.84	8.89	0.69
Ψ , %	0.00	0.00	0.00	7.85	12.96	0.57
Π , %	32.05	27.61	30.12	25.24	19.25	27.32
ρ , g/cm ³	5.58	6.21	6.09	6.32	6.64	6.22
HRB	70.4	90.4	67	74.2	59.1	74.1

In the specimens obtained from a mixture of ferrochrome, iron powders with copper and nickel additives, even after sintering in vacuum, the relative elongation δ and relative contraction Ψ do not exceed 1 % (Table 2). Therefore, in calculations, the yield strength of all steels under study, in which δ and Ψ are less than 1–2 %, was assumed to be equal to the strength limit.

Since the plastic properties of steels are influenced not only by chemical composition and structure, but also by the stress-strain state, radial settling of sintered ring specimens with residual porosity of 14–25 % was carried out to evaluate σ_s . It was found that in the compression zones the relative density during upsetting increases to 0.95–0.97 and cracks appear only in the tensile zones. Taking this into account, $\sigma_s = 200$ MPa was taken in the calculations.

To determine the contact stresses τ_c and the friction coefficient, we used the method of transverse deformation of the sintered blank using a punch with different diameters (Fig. 10). The initial height of the sintered ring blanks was 14.5 mm, outer diameter was 25 mm, wall thickness (h_r) was 2.75 mm.

Before testing, lubricants in the form of suspensions consisting of graphite, molybdenum disulfide and polytetrafluoroethylene (PTFE) particles were applied to the inner surface of the sintered blanks. As an example, Fig. 11 shows the effect of lubricant composition on the work (A_d) and transverse deformation resistance (P_d) of a 304L-AW-100 powder blank with an initial porosity of 17 % at a relative radial strain $\varepsilon_r = 0.24$.

The minimum resistance to transverse deformation of the porous blank at $\varepsilon_r = 0.24$ was obtained in the case of coating the inner surface of the billet with PTFE (Fig. 11, *b*, curve 3). The maximum strain resistance in all cases was obtained at 12–14 mm displacement of the punch. With increasing degree of radial deformation P_d smoothly increases from 0.5 to 45–50 kN, and at $\varepsilon_r \geq 0.24$ –0.25 the force of deformation resistance increases more intensively (Fig. 12).

It should be noted that regardless of the composition of lubricants, the strength of resistance to transverse deformation of the workpiece at $\varepsilon_r \leq 0.24$ –0.25, determined experimentally and by simulating using the *QForm* program, practically does not differ (Fig. 12).

Let us assume that the work of friction forces on the contact surface of the blank with the matrix is much less than on the punch-blank surface (Fig. 10, *a*). Then on the inner surface of the blank the elementary work dA of tangential forces in the deformation center with height dh [21]

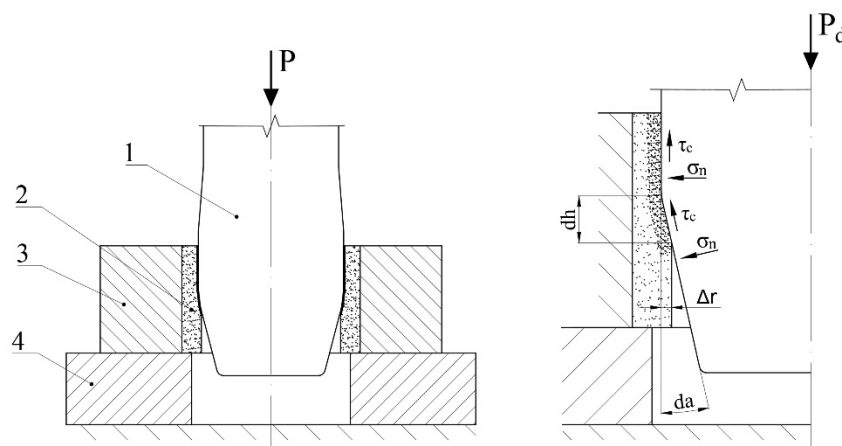


Fig. 10. Scheme of radial deformation for determining contact stresses:

1 – punch; 2 – annular specimen; 3 – matrix; 4 – stand

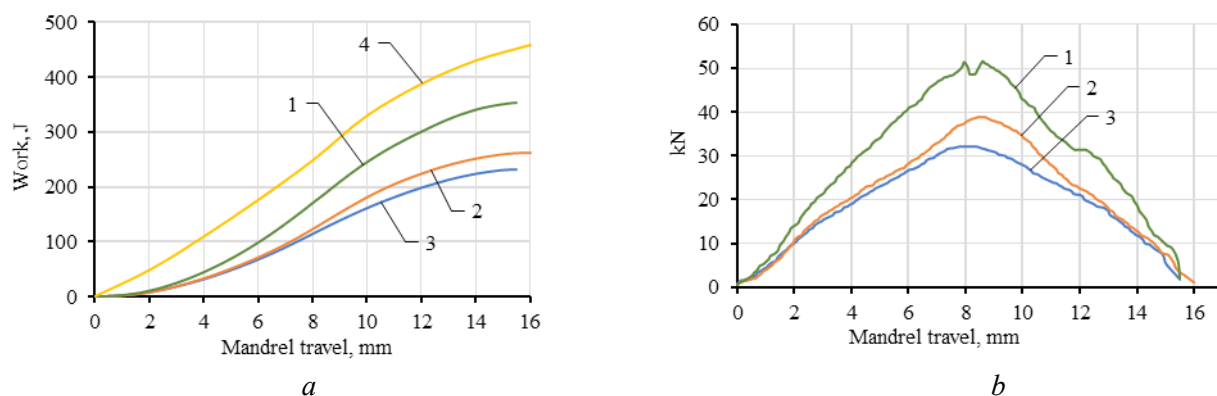


Fig. 11. Dependence of energy (*a*) and resistance to transverse strain (*b*) of the sintered blank at $\Delta r = 0.65$ mm on the lubricant composition:

1 and 4 – pencil graphite; 2 – MoS_2 ; 3 – PTFE

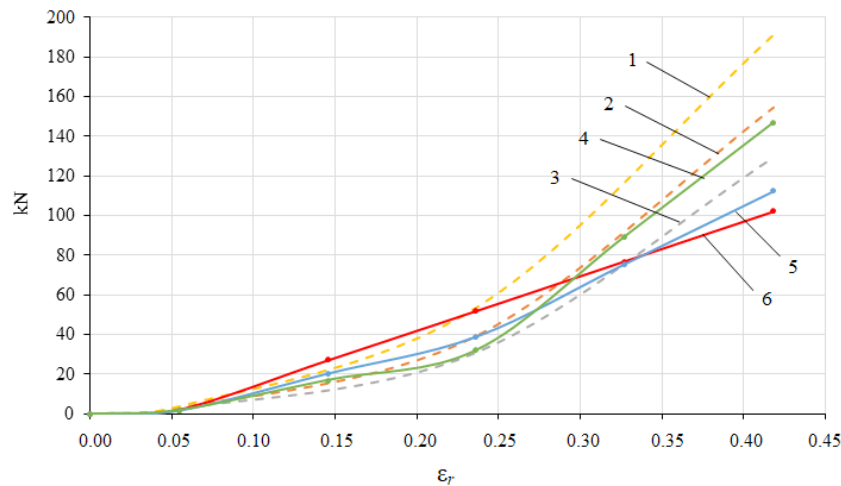


Fig. 12. Strain resistance under radial deformation of a ring specimen with porosity 17 %:

dotted line – simulation data; solid line – natural data 1 – soap solution; 2 – graphite + oil; 3 – phosphate + soap; 4 – PTFE + oil; 5 – MoS_2 + oil; 6 – graphite + oil

$$dA = \tau_c r d\alpha = \sigma_s \mu_c r d\alpha = \frac{1}{2} \sigma_s \mu_c h \varepsilon_r^2, \quad (12)$$

where σ_s is the yield strength of the workpiece material; μ_c is the contact friction coefficient; r is the inner radius of the powder workpiece after radial deforming; α is the punch cone angle.

From expression (12) we find:

$$\mu_c = \frac{2dA_d}{\sigma_s r h_r \varepsilon_r^2}. \quad (13)$$

Since in the process of radial deformation the work and the strain resistance force depend on the relative degree of radial deformation and the displacement of the punch (Fig. 11, b), for each value of h_r the coefficient of contact friction for the given values of the yield strength of the material was determined by formula (13). In particular, Fig. 13 shows the influence of the degree of radial deformation ε_r of vacuum sintered ring specimens with porosity of 17 % from 304L-AW-100 powder, depending on the composition of lubricant and punch displacement on the coefficient of contact friction.

Similarly, we determined the work of friction forces on the inner contact surface as a result of moving the punch along the entire height of the blank by the following equation:

$$A_c = \sigma_s \mu_c (\Delta r)^2 h_r \sin^2 \frac{\alpha}{2}. \quad (14)$$

Formulas (13) and (14) do not take into account the effect of blank porosity on the contact friction coefficient at all stages of transverse deformation. As can be seen from (Fig. 13, d), μ_c will be influenced not only by the initial porosity of the blank, but also by the nature of its height distribution, as well as by the concentration of solid lubricant particles located in open pores.

The strain energy calculated by formula (10), using the results of experimental studies μ_c (Fig. 13, b curve 1), is noticeably greater than determined experimentally (Fig. 11, a). Therefore, depending on the design, operating conditions, technological properties of antifriction and lubricating materials we recommend to use the variant of sintered blanks design developed by the authors and methods of calculation of energy-force parameters, creation of new technology for obtaining non-displacement spherical sliding bearings. The results of research can be used in the development of technology for cold and hot die forging of powdered parts from other materials, as well as in the calibration of sintered blanks.

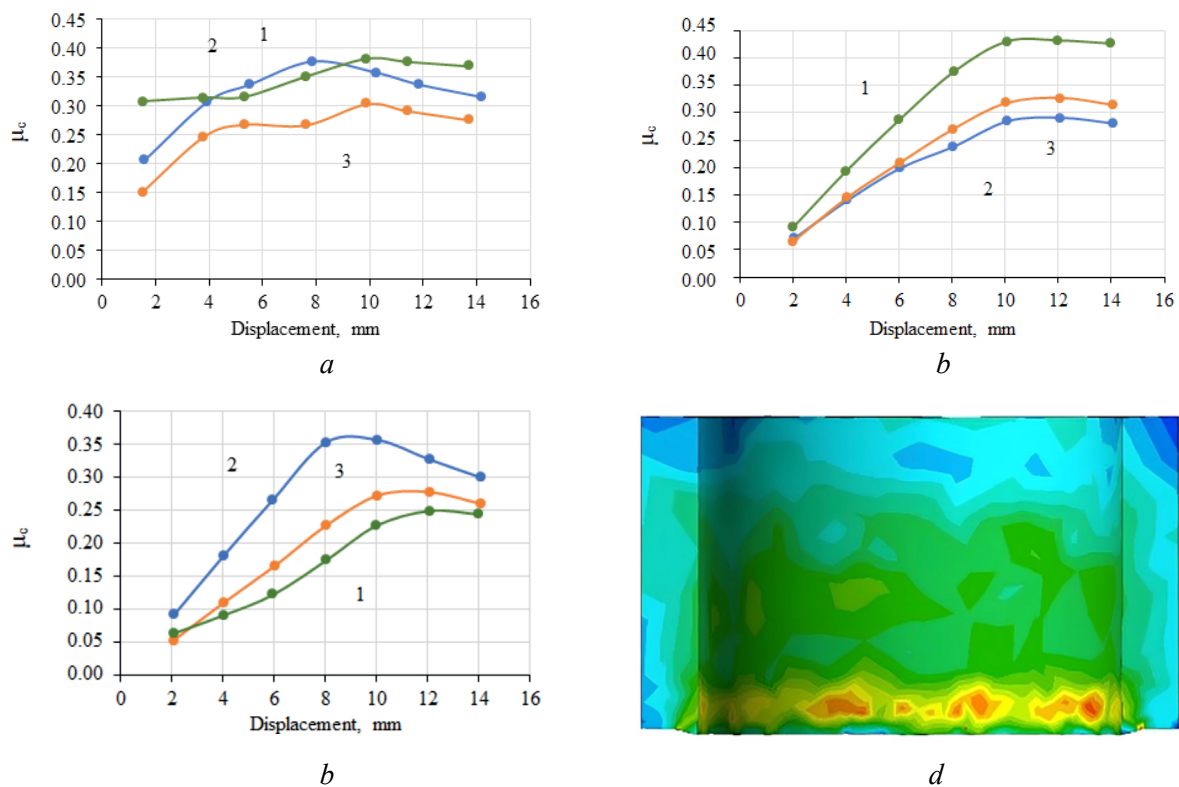


Fig. 13. Dependence of the coefficient of contact friction during radial deformation of an annular specimen on the degree of transverse strain ($\epsilon_r = 0.05$ (a); $\epsilon_r = 0.24$ (b), $\epsilon_r = 0.42$ (c)) and lubricant composition:

1 – pencil graphite; 2 – PTFE; 3 – MoS_2

Conclusion

1. It is experimentally proved that the strain resistance and strain energy, as well as the density of the spherical sliding bearing ring made of corrosion-resistant steel powders, obtained by cold forming of sintered blanks, are influenced by the configuration of the end surface of punches. The top and bottom edges are most intensively compacted when the punch faces are made with a chamfer angle of 30–40 deg.

2. It is established that in the production of one-piece spherical sliding bearings it is advisable to use sintered cylindrical blanks coated with lubricants containing solid particles of molybdenum disulfide and polytetrafluoroethylene, which makes it possible to reduce the strain resistance during cold forming of the outer ring by 20–30 %, and the sliding friction coefficient during operation is within 0.05–0.06.

3. It is revealed that mechanical and technological properties of sintered blanks from chromium-nickel stainless steels are influenced not only by the chemical composition of powders, but also by the mode and conditions of press sintering. The ultimate strength of specimens sintered in vacuum is 230–240 MPa, and in dissociated ammonia the ultimate strength is 40–45 MPa due to intensive oxidation of chromium on the boundaries of powder particles not only by oxygen contained in the protective environment, but also with oxygen slammed in the pores of the blank.

4. A simpler method of calculated and experimental determination of the contact friction coefficient is developed, which makes it possible to evaluate the influence of the degree and work of deformation, composition of lubricants containing solid particles of molybdenum disulfide and PTFE on the kinetics of forming at obtaining parts of various configurations by cold die forging of porous blanks.

References

1. Dorofeev Yu.G., Gasanov B.G., Dorofeev V.Yu., Mishchenko V.N., Miroshnikov V.I. *Promyshlennaya tekhnologiya goryachego pressovaniya poroshkovykh izdelii* [Industrial technology of hot pressing of powder products]. Moscow, Metallurgiya Publ., 1990. 206 p. EDN: OFSEDO.



2. Kuhn H.A., Downey C.L. Material behavior in powder preform forging. *Journal of Engineering Materials and Technology*, 1973, vol. 95 (1), pp. 41–46. DOI: 10.1115/1.3443104.

3. Gorokhov V.M., Doroshkevich E.A., Efimov A.M., Zvonarev E.V. *Ob''emnaya shtampovka poroshkovykh materialov* [Volumetric punching of powder materials]. Minsk, Navuka i tekhnika Publ., 1993. 272 p. ISBN 5-343-00895-X.

4. Vorontsov A.L. Account for the nonuniformity of the mechanical properties and the deformation rate in the calculations of the pressure working processes. *Russian Engineering Research*, 2003, vol. 23 (6), pp. 62–69. EDN: DJBLGD.

5. Skorokhod G.E., Burnaev N.I., Kortsenshtein N.E., Burnov A.M., Serdyuk G.G. Tekhnologicheskie osobennosti izgotovleniya detalei slozhnoi formy iz metallicheskih poroshkov metodom goryachei shtampovki [Technological peculiarities of manufacturing complex-shaped parts from metal powders by hot stamping method]. *Poroshkovaya metallurgiya = Powder metallurgy*, 1988, no. 3, pp. 29–33.

6. Oyane M., Shima S., Tabata T. Consideration of basic equations, and their application, in the forming of metal powders and porous metals. *Journal of Mechanical Working Technology*, 1978, vol. 1 (4), pp. 325–341. DOI: 10.1016/0378-3804(78)90036-0.

7. Green R.J. A plasticity theory for porous solids. *International Journal of Mechanical Sciences*, 1972, vol. 14 (4), pp. 215–224. DOI: 10.1016/0020-7403(72)90063-X.

8. Oyane M., Shima S., Kono Y. Theory of plasticity porous metals. *Bulletin of JSME*, 1973, vol. 16 (99), pp. 1254–1262. DOI: 10.1299/jsme1958.16.1254.

9. Baglyuk G.A., Yurchuk V.A., Kovalenko S.S. Primenenie variatsionnykh metodov dlya rascheta protsessov obrabotki davleniem spechennykh zagotovok [Application of variational methods for calculation of pressure treatment processes of sintered workpieces]. *Fizika i tekhnika vysokikh davlenii = Physics and high pressure technology*, 1987, vol. 24, pp. 57–61.

10. Shima S., Oyane M. Plasticity theory for porous metals. *International Journal of Mechanical Sciences*, 1976, vol. 18 (6), pp. 285–291. DOI: 10.1016/0020-7403(76)90030-8.

11. Kuhn H.A., Downey C.L. Deformation characteristics and plasticity theory of sintered powder materials. *International Journal of Powder Metallurgy*, 1971, vol. 7 (1), pp. 15–25.

12. Rozenberg O.A., Mikhailov O.V., Shtern M.B. Chislennoe modelirovanie protsessa deformatsionnogo uprochneniya poroshkovykh vtulok metodom mnogokratnogo protyagivaniya [Strain hardening of porous bushings by multiple mandreling: numerical simulation]. *Poroshkovaya metallurgiya = Powder metallurgy*, 2012, no. 7–8, pp. 4–11.

13. Kondo H., Hegedus M. Current trends and challenges in the global aviation industry. *Acta Metallurgica Slovaca*, 2020, vol. 26 (4), pp. 141–143. DOI: 10.36547/ams.26.4.763.

14. Laptev A.M. Postroenie deformatsionnoi teorii plastichnosti poristyykh materialov [Construction of deformation theory of plasticity of porous materials]. *Izvestiya vysshikh uchebnykh zavedenii. Mashinostroyeniye = Proceedings of Higher Educational Institutions. Machine Building*, 1980, no. 4, pp. 153–156.

15. Koval'chenko M.S. Deformatsionnoe uprochnenie poroshkovogo tela pri pressovanii [Strain hardening of a powder body in pressing]. *Poroshkovaya metallurgiya = Powder metallurgy*, 2009, no. 3–4, pp. 13–27.

16. Sobotka Z. The plastic flow orthotropic materials with different mechanical properties in tension and compression. *Acta Technica CSAV*, 1971, no. 6, pp. 772–776.

17. Laptev A.M. Kriterii plastichnosti poristyykh metallov [Plasticity criteria for porous metals]. *Poroshkovaya metallurgiya = Powder metallurgy*, 1982, no. 7, pp. 12–18.

18. Xin X.J., Jayaraman P., Daehn G.S., Wagoner R.H. Investigation of yield surface of monolithic and composite powders by explicit finite element simulation. *International Journal of Mechanical Sciences*, 2003, vol. 45 (4), pp. 707–723. DOI: 10.1016/S0020-7403(03)00107-3.

19. Vlasov A.V., Stebunov S.A., Evsyukov S.A., Biba N.V., Shitikov A.A. *Konechno-elementnoe modelirovanie tekhnologicheskikh protsessov kovki i ob''emnoi shtampovki* [Finite element modeling of technological processes of forging and volume stamping]. Moscow, Bauman MSTU Publ., 2019. 383 p. ISBN 978-5-7038-5101-2.

20. Gromov N.P. *Teoriya obrabotki metallov davleniem* [Theory of metal forming by pressure]. Moscow, Metallurgiya Publ., 1978. 360 p.

21. Storozhev M.V., Popov E.A. *Teoriya obrabotki metallov davleniem* [Theory of metal forming by pressure]. Moscow, Mashinostroyeniye Publ., 1977. 423 p. EDN: XSGYCB.



22. Perlin I.L., Raitborg L.Kh. *Teoriya pressovaniya metallov* [Theory of metal pressing]. Moscow, Metallurgiya Publ., 1975. 442 p.

23. Baglyuk G.A. Analiz kinematiki svobodnoi osadki poristogo tsilindra s uchetom kontaktnogo treniya [Analysis of the kinematics of the process of free upsetting of a porous cylinder in the presence of contact friction]. *Poroshkovaya metallurgiya = Powder metallurgy*, 1993, no. 1, pp. 17–21.

Conflicts of Interest

The authors declare no conflict of interest.

© 2024 The Authors. Published by Novosibirsk State Technical University. This is an open access article under the CC BY license (<http://creativecommons.org/licenses/by/4.0>).